

Photoproduction of J/ψ in p-p ultra-peripheral collisions at LHC energy

Zhi-Lei Ma^{a,c}, Zhun Lu^b, Jia-Qing Zhu^{a,*}, Li Zhang^{c,*}

^a*Department of Physics, Yunnan University, Kunming, 650091, China*

^b*School of Physics, Southeast University, Nanjing, 211189, China*

^c*Department of Astronomy, Key Laboratory of Astroparticle Physics of Yunnan Province, Yunnan University, Kunming, 650091, China*

Abstract

J/ψ production in p-p ultra-peripheral collisions through the elastic and inelastic photoproduction processes, where the virtual photons emitted from the projectile interact with the target, are studied. The comparisons between the exact treatment results and the ones of equivalent photon approximation are expressed as Q^2 (virtuality of photon), z and p_T distributions, and the total cross sections are also estimated. The method developed by Martin and Ryskin is employed to avoid double counting when the different production mechanism are considered simultaneously. The numerical results indicate that, the equivalent photon approximation can be only applied to the coherent or elastic electromagnetic process, the improper choice of Q_{\max}^2 and y_{\max} will cause obvious errors. And the exact treatment is needed to deal accurately with the J/ψ photoproduction.

1. Introduction

It is well known that the photoproduction processes in ultra-peripheral collisions (UPCs) can be theoretically studied by using the equivalent photon approximation (EPA), which can be traced back to early works by Fermi [1], Weizsäcker and Williams [2], and Landau and Lifshitz [3, 4]. The central idea of EPA is that the electromagnetic field of a fast moving charged particle can

*Corresponding author

Email addresses: mz10197@ynu.edu.cn (Zhi-Lei Ma), zhujiaqing@ynu.edu.cn (Jia-Qing Zhu), lizhang@ynu.edu.cn (Li Zhang)

be interpreted as an equivalent flux of photon distributed with some density $n(\omega)$ on a frequency spectrum [5–7]. Thus, the cross section is approximated by the convolution of the photon flux with the relevant real photoproduction cross section. Since its convenience and simplicity, EPA has been widely applied to many topics, for instance, heavy quarkonium photoproduction, two-photon particle production, the determination of the nuclear parton distributions, and small- x physics. [8–20]. EPA is sensitive to the value of kinematical variables, and can only be employed in the very restricted kinematical regions and in some special processes [13]. In most of physically interesting cases, the EPA accuracy is usually denoted by a dynamical cut off Λ_γ^2 of the photon virtuality Q^2 . At $Q^2 < \Lambda_\gamma^2$, virtual photo-absorption cross sections differ slightly from their values on the mass shell and quickly decrease at $Q^2 > \Lambda_\gamma^2$. Thus, EPA is a reasonable approximation comparing with the exact treatment, and is used precisely for the description of the cross sections only at $Q^2 < \Lambda_\gamma^2$ [17–19]. However, the applicability range of EPA and of its accuracy are not always considered in most works where the improper bounds of involved variables are used, such as Q_{\max}^2 is usually set as $\hat{s}/4$ (\hat{s} is the squared centre-of-mass (CM) frame energy of the photo-absorption processes) or even infinity, $y_{\max} = 1$ are also adopted directly, and a number of imprecise statements and some widely used equivalent photon spectra are obtained beyond the EPA validity range [16–26]. Furthermore, when the different types of photoproduction processes are considered, the serious double counting exist which will cause the results include the large fictitious contributions.

In this work, we consider the photoproduction of J/ψ in p-p UPCs at LHC energy, which has received many researches in EPA. We present the comparisons between EPA and the exact treatment which reduces to the EPA in the limit $Q^2 \rightarrow 0$ and can be considered as the generalization of Lep-toproduction [27–29]. Actually, as always with photons, the situation is quite complex. We have to deal with the several kinds of interactions simultaneously, and the method developed by Martin and Ryskin [30] is adopted to avoid double counting. There are two types of photon emission mechanisms should be distinguished [9, 31]: coherent and incoherent emissions. In the first type, virtual photon are radiated coherently by the whole proton which remains intact after the photon emitted. In the second type, virtual photon are radiated incoherently by the charged constituents inside the proton, and the proton will dissociate or excite after the photon emitted. Otherwise, two kinds of photoproduction mechanisms need to be considered: elastic and

inelastic reactions. In the first case, a certain particle is produced while the target remains in the ground state (or is only internally excited). On the other hand, in the inelastic interactions the particle produced is accompanied by one or more particles from the breakup of the target.

This paper is organized as follow. Section 2 presents the formalism of exact treatment for the J/ψ photoproduction in p-p UPCs. Based on the method of Martin and Ryskin, the coherent and incoherent contributions, and the elastic and inelastic interactions are considered simultaneously. EPA is also introduced by taking $Q^2 \rightarrow 0$ in the exact treatment. Section 3 illustrates the numerical results, the distributions of Q^2 , z and p_T , and the total cross sections are presented. Finally, the summary and conclusions are given in Section 4. To avoid confusion, the terminology "coherent" or "incoherent" is always used to describe the photon emission types in this paper, which is different in many literatures where the "coherent" and "incoherent" usually refer to the case that the target nucleus remains intact or break up after scattering with photon.

2. Formalism

Heavy quarkonium production involves both perturbative and nonperturbative aspects of quantum chromodynamics (QCD), which can be calculated by using the nonrelativistic QCD (NRQCD) factorization formalism [32]. This formalism implies a separation of short-distance coefficients, which can be calculated perturbatively as expansions in the strong-coupling constant α_s , from long-distance matrix elements (LDMEs), which must be extracted from experiment. The LDMEs are process independent, and can be classified in terms of their scaling in ν , the relative velocity of the heavy quarks in the bound state. A crucial feature for this formalism is that it takes into account the $Q\bar{Q}$ Fock space, which is spanned by the states $n = {}^{2S+1}L_J^{(c)}$ with definite spin S , orbital angular momentum L , total angular momentum J , and color multiplicity c . In particular, this formalism predicts the existence of color-octet processes by the nonperturbative emission of soft gluons in nature.

In this section, we employ the NRQCD factorization formalism to describe the inelastic J/ψ photoproduction. And for elastic interactions, we adopt a general method of high energy scattering developed by Dosch and Ferreira [33–36], which based on the functional integral approach [37, 38] to QCD and on the WKB method. This approach is capable of incorporating both the

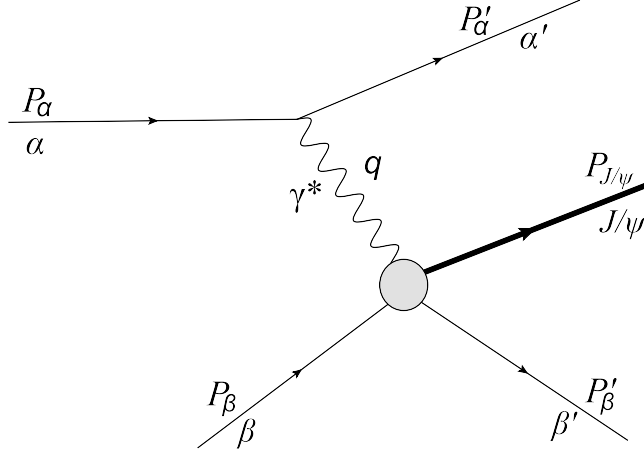


Figure 1: The J/ψ photonproduction in ultra-peripheral p-p collision. The virtual photon emitted from the projectile α interacts with target β , α can be the proton or it's charged parton for coherent and incoherent photon emissions mechanisms, respectively. And β can also be the proton or it's parton (quark or gluon) for elastic and inelastic interactions, respectively. α' and β' are the scattered α and β , respectively.

perturbative and nonperturbative aspects. The functional integrals are calculated nonperturbatively, in an extended stochastic vacuum model [39, 40], that has been successfully applied in many fields, from hadron spectroscopy to high energy scattering.

2.1. Exact treatment

As a generalization of Leptoproduction framework, the exact treatment for the J/ψ photoproduction in p-p UPCs is based on the expansion of the proton or quark tensor (multiplied by Q^{-2}) by using the transverse and longitudinal polarization operators, and thus the virtual photon radiated from the projectile is off mass shell and no longer transversely polarized. The formalism is analogous with Ref. [29].

The general form of cross section for J/ψ photoproduction in p-p UPCs, which is described in Fig. 1, can be written as

$$\begin{aligned}
 d\sigma(\alpha + \beta \rightarrow \alpha + J/\psi + \beta) &= \frac{|\mathcal{M}_{\alpha\beta}|^2}{4p_{\text{CM}}\sqrt{s_{\alpha\beta}}} d\text{PS}_3(p_\alpha + p_\beta; p'_\alpha, J/\psi, p'_\beta) \\
 &= \frac{|\mathcal{M}_{\alpha\beta}|^2}{4p_{\text{CM}}\sqrt{s_{\alpha\beta}}} \frac{d^3 p'_\alpha}{(2\pi)^3 2E'_\alpha} d\text{PS}_2(q + p_\beta; J/\psi, p'_\beta),
 \end{aligned}$$

(1)

where $d\text{PS}_3(p_\alpha + p_\beta; p'_\alpha, J/\psi, p'_\beta)$ is the Lorentz-invariant phase-space measure. $p_{\text{CM}} = \sqrt{(s_{\alpha\beta} - m_\alpha^2 - m_\beta^2)^2 - 4m_\alpha^2 m_\beta^2} / 2\sqrt{s_{\alpha\beta}}$ and $s_{\alpha\beta} = (p_\alpha + p_\beta)^2$ are the momentum and energy square of $\alpha\beta$ CM frame, respectively. E'_α is the energy of the scattered projectile α .

To obtain the Q^2 distribution, it is convenient to do the calculations in the rest frame of α , where $|\mathbf{q}| = |\mathbf{p}_{\alpha'}| = r$, $Q^2 = -q^2 = (p_\alpha - p_{\alpha'})^2 = 2m_\alpha(\sqrt{r^2 + m_\alpha^2} - m_\alpha)$, $d^3p'_\alpha = r^2 dr d\cos\theta d\varphi$, and $y = (q \cdot p_\beta) / (p_\alpha \cdot p_\beta) = (q_0 - |\mathbf{p}_\beta| r \cos\theta / E_\beta) / m_\alpha$. By using the Jacobian determinant,

$$dydQ^2 = \left| \frac{D(Q^2, y)}{D(\cos\theta, r)} \right| d\cos\theta dr = \frac{2|\mathbf{p}_\beta| r^2}{E_{\alpha'} E_\beta} d\cos\theta dr, \quad (2)$$

where $E_\beta = (s_{\alpha\beta} - m_\alpha^2 - m_\beta^2) / 2m_\alpha$, the cross section of subprocess $\alpha + \beta \rightarrow \alpha + J/\psi + \beta$ can be expressed as

$$\begin{aligned} & d\sigma(\alpha + \beta \rightarrow \alpha + J/\psi + \beta) \\ &= \frac{e_\alpha^2 \alpha}{Q^2} \frac{y \rho^{\mu\nu} T_{\mu\nu}}{8\pi^2} \frac{d\text{PS}_2(q + p_\beta; J/\psi, p'_\beta)}{4\hat{p}_{\text{CM}} \sqrt{\hat{s}}} f(s_{\alpha\beta}, p_{\text{CM}}, \hat{s}, \hat{p}_{\text{CM}}, m_\alpha, m_\beta) dydQ^2 d\varphi, \end{aligned} \quad (3)$$

where e_α is the charge of projectile, $\alpha = 1/137$ is the electromagnetic coupling constant, \hat{p}_{CM} and $\hat{s} = (q + p_\beta)^2$ are the momentum and energy square of $\gamma^* \beta$ CM frame, and

$$f(s_{\alpha\beta}, p_{\text{CM}}, \hat{s}, \hat{p}_{\text{CM}}, m_\alpha, m_\beta) = \frac{\hat{p}_{\text{CM}} \sqrt{\hat{s}}}{y p_{\text{CM}} \sqrt{s_{\alpha\beta}}} \frac{s_{\alpha\beta} - m_\alpha^2 - m_\beta^2}{\sqrt{(s_{\alpha\beta} - m_\alpha^2 + m_\beta^2)^2 - 4m_\alpha^2 m_\beta^2}}, \quad (4)$$

the decomposition $|\mathcal{M}_{\alpha\beta}|^2 = 4\pi\alpha^2 e_\alpha^2 \rho^{\mu\nu} T_{\mu\nu} / Q^2$ is used, $T_{\mu\nu}$ is the amplitude of reaction $\gamma^* + \beta \rightarrow J/\psi + \beta$, and $\rho^{\mu\nu}$ is the tensor of projectile α (multiplied by Q^{-2})

$$\rho^{\mu\nu} = (-g^{\mu\nu} + \frac{q^\mu q^\nu}{q^2}) F_2(Q^2) - \frac{(2P_\alpha - q)^\mu (2P_\alpha - q)^\nu}{q^2} F_1(Q^2), \quad (5)$$

$F_1(Q^2)$ and $F_2(Q^2)$ are the general expressions of form factors for the projectile α .

With the help of the linear combinations [13]

$$Q^\mu = \sqrt{\frac{-q^2}{(q \cdot p_\beta)^2 - q^2 p_\beta^2}} (p_\beta - q \frac{q \cdot p_\beta}{q^2})^\mu,$$

$$R^{\mu\nu} = -g^{\mu\nu} + \frac{(q \cdot p_\beta)(q^\mu p_\beta^\nu + q^\nu p_\beta^\mu) - q^2 p_\beta^\mu p_\beta^\nu - p_\beta^2 q^\mu q^\nu}{(q \cdot p_\beta)^2 - q^2 p_\beta^2},$$

they satisfy the relations: $q_\mu Q^\mu = q_\mu R^{\mu\nu} = 0$, $Q^\mu Q_\mu = 1$, $\rho^{\mu\nu}$ can be expanded as

$$\rho^{\mu\nu} = \rho^{00} Q^\mu Q^\nu + \rho^{++} R^{\mu\nu}, \quad (6)$$

where $\rho^{++} = R^{\mu\nu} \rho_{\mu\nu}/2$, $\rho^{00} = Q^\mu Q^\nu \rho_{\mu\nu}$. It can be seen that $R^{\mu\nu}$ and $Q^\mu Q^\nu$ are equivalent to the transverse and longitudinal polarizations [29]: $R^{\mu\nu} = \varepsilon_T^{\mu\nu}$, $Q^\mu Q^\nu = -\varepsilon_L^{\mu\nu}$, respectively. On the other hand, we adopt Martin-Ryskin method by using the weighting factor P_β to distinguish the different part in the whole processes [30]. Thus, the differential cross section of subprocess $\alpha + \beta \rightarrow \alpha + J/\psi + \beta$ can accordingly be expressed as

$$\begin{aligned} & \frac{d\sigma}{dydQ^2}(\alpha + \beta \rightarrow \alpha + J/\psi + \beta) \\ &= \frac{e_\alpha^2 \alpha}{2\pi} \frac{1}{2} \left(\frac{y\rho^{++}}{Q^2} R^{\mu\nu} T_{\mu\nu} + \frac{y\rho^{00}}{Q^2} Q^\mu Q^\nu T_{\mu\nu} \right) P_\beta f(s_{\alpha\beta}, p_{\text{CM}}, \hat{s}, \hat{p}_{\text{CM}}, m_\alpha, m_\beta) \\ & \quad \times \frac{d\text{PS}_2(q + p_\beta; J/\psi, p'_\beta)}{4\hat{p}_{\text{CM}}\sqrt{\hat{s}}} \\ &= dt \frac{e_\alpha^2 \alpha}{2\pi} \left[\frac{y\rho^{++}}{Q^2} \frac{d\sigma_T}{dt}(\gamma^* + \beta \rightarrow J/\psi + \beta) + \frac{y\rho^{00}}{Q^2} \frac{d\sigma_L}{2dt}(\gamma^* + \beta \rightarrow J/\psi + \beta) \right] \\ & \quad \times P_\beta f(s_{\alpha\beta}, p_{\text{CM}}, \hat{s}, \hat{p}_{\text{CM}}, m_\alpha, m_\beta), \end{aligned} \quad (7)$$

where the relations

$$\begin{aligned} d\sigma_T(\gamma^* + \beta \rightarrow J/\psi + \beta) &= \frac{1}{2} R^{\mu\nu} T_{\mu\nu} \frac{d\text{PS}_2(q + p_\beta; J/\psi, p'_\beta)}{4\hat{p}_{\text{CM}}\sqrt{\hat{s}}}, \\ d\sigma_L(\gamma^* + \beta \rightarrow J/\psi + \beta) &= Q^\mu Q^\nu T_{\mu\nu} \frac{d\text{PS}_2(q + p_\beta; J/\psi, p'_\beta)}{4\hat{p}_{\text{CM}}\sqrt{\hat{s}}}, \end{aligned} \quad (8)$$

are used, and

$$\rho^{++} = F_2(Q^2) + \frac{1}{2} \left[\frac{(2-y)^2}{y^2 + Q^2 m_p^2 / (p_\alpha \cdot p_\beta)^2} - \frac{4m_\alpha^2}{Q^2} - 1 \right] F_1(Q^2),$$

$$\rho^{00} = -F_2(Q^2) + \frac{(2-y)^2}{y^2 + Q^2 m_p^2 / (p_\alpha \cdot p_\beta)^2} F_1(Q^2). \quad (9)$$

Here, $d\sigma_T/d\hat{t}$ and $d\sigma_L/d\hat{t}$ represent the transverse and longitudinal cross sections of subprocess $\gamma^* + \beta \rightarrow J/\psi + \beta$, respectively.

For the elastic reactions, the weighting factor in Eq. (7) is chosen as $P_\beta = G_E^2(Q^2)$ for recognizing the elastic part from the whole processes, where G_E is the elastic form factor of proton and can be parameterized by the dipole form

$$G_E(Q^2) = \frac{1}{(1 + Q^2/0.71 \text{ GeV})^2}. \quad (10)$$

And we adopt a general method developed by Dosch and Ferreira, in terms of the overlaps of the photon and vector meson light cone wave functions, the production amplitude of vector mesons can be written as

$$\begin{aligned} & T_{\gamma^* p \rightarrow V p, \lambda}(\hat{t}) \\ &= \int d^2 R_1 dz_1 \psi_{V\lambda}(z_1, R_1)^* \psi_{\gamma^*\lambda}(z_1, R_1, Q^2) J(\mathbf{q}, z, \mathbf{R}_1) \\ &\approx (-2is) \frac{C e^{-a|\hat{t}|}}{1 + b|\hat{t}|} \exp\left[\frac{-12\eta|\hat{t}|}{Q^2 + M_V^2}\right] \left(T_h^\lambda(Q^2) \left(\frac{\hat{s}}{s_0}\right)^{\epsilon_h} + T_s^\lambda(Q^2) \left(\frac{\hat{s}}{s_0}\right)^{\epsilon_s} \right), \end{aligned} \quad (11)$$

the details can be found in Refs. [33–36]. Thus, the transverse and longitudinal cross sections of subprocess $\gamma^* + p \rightarrow J/\psi + p$ can be cast into

$$\frac{d\sigma_{T(L)}}{d\hat{t}}(\gamma^* + p \rightarrow J/\psi + p) = \frac{1}{16\pi \hat{s}^2} |T_{\gamma^* p \rightarrow J/\psi p}^{\pm(0)}|^2, \quad (12)$$

where the helicities $\lambda = \pm 1$ and 0 denote the transverse and longitudinal polarizations of the photon. Considering the different photon emission mechanisms, the elastic J/ψ photoproduction should be divided into the elastic-coherent (el-coh.) and elastic-incoherent (el-incoh.) processes. In the elastic-coherent process, virtual photon radiated coherently by the whole incident proton interacts with the another incident proton, and proton remains intact after scattering. The cross section of J/ψ produced by this channel is

$$\frac{d\sigma^{\text{el-coh.}}}{dQ^2}(p + p \rightarrow p + J/\psi + p) = \int dy \frac{d\sigma}{dy dQ^2}(p + p \rightarrow p + J/\psi + p). \quad (13)$$

$d\sigma/dy dQ^2(p + p \rightarrow p + J/\psi + p)$ can be obtained from Eqs. (7) and (12), where both the projectile and target are the proton: $m_\alpha = m_\beta = m_p$, and the general expressions of form factor $F_1(Q^2)$ and $F_2(Q^2)$ turn into the elastic proton form factors $H_1(Q^2)$ and $H_2(Q^2)$ accordingly. Then the proton tensor multiplied by Q^{-2} reads

$$\begin{aligned}\rho_{\text{el-coh.}}^{++} &= H_2(Q^2) + \frac{1}{2} \left[\frac{(y-2)^2}{y^2 + Q^2 m_p^2 / (p_\alpha \cdot p_\beta)^2} - \frac{4m_p^2}{Q^2} - 1 \right] H_1(Q^2), \\ \rho_{\text{el-coh.}}^{00} &= -H_2(Q^2) + \frac{(y-2)^2}{y^2 + Q^2 m_p^2 / (p_\alpha \cdot p_\beta)^2} H_1(Q^2),\end{aligned}\quad (14)$$

where

$$\begin{aligned}H_1(Q^2) &= \frac{G_E^2(Q^2) + (Q^2/4m_p^2)G_M^2(Q^2)}{1 + Q^2/4m_p^2}, \\ H_2(Q^2) &= G_M^2(Q^2) = 2.79^2 G_E^2(Q^2),\end{aligned}\quad (15)$$

In the Martin-Ryskin method [30], the coherent probability, or weighting factors (WF), is given by the square of the form factor $G_E^2(Q^2)$, while the effect of magnetic form factor is neglected

$$H_1(Q^2) = H_2(Q^2) = G_E^2(Q^2). \quad (16)$$

This approximation has been widely applied for the derivation of the equivalent photon fluxes of proton, such as the photon spectrum Eq.(34) that we will discuss in section 2.3, which developed by Drees and Zeppenfeld [18]. However, in the present paper, we take into account the complete expressions given in Eq. (15).

In the elastic-incoherent processes, virtual photon, emitted from quarks inside incoming proton, interacts with the target proton which remains intact after scattering. Accordingly, the cross section of J/ψ produced by el-incoh. is

$$\begin{aligned}& \frac{d\sigma^{\text{el-incoh.}}}{dQ^2}(p + p \rightarrow X_A + J/\psi + p) \\ &= \sum_a \int dy dx_a f_{a/p}(x_a, \mu^2) \frac{d\sigma}{dy dQ^2}(a + p \rightarrow a + J/\psi + p),\end{aligned}\quad (17)$$

where $x_a = p_a/p_A$ is the parton's momentum fraction, $f_{a/p}(x_a, \mu^2)$ is the parton distribution function of proton A, and the factorized scale is chosen

as $\mu = \sqrt{m_{J/\psi}^2 + Q^2}$, the cross section $d\sigma/dydQ^2(a + p \rightarrow a + J/\psi + p)$ can also be obtained from Eqs. (7) and (12) with $m_\alpha = m_a = 0$, $m_\beta = m_p$. And $F_1(Q^2) = F_2(Q^2) = L_1(Q^2) = L_2(Q^2)$, then the massless quark tensor multiplied by Q^{-2} is

$$\begin{aligned}\rho_{\text{el-incoh.}}^{++} &= L_2(Q^2) - \frac{1}{2} \left[1 - \frac{(y-2)^2}{y^2 + Q^2 m_p^2 / (p_\alpha \cdot p_\beta)^2} \right] L_1(Q^2), \\ \rho_{\text{el-incoh.}}^{00} &= -L_2(Q^2) + \frac{(y-2)^2}{y^2 + Q^2 m_p^2 / (p_\alpha \cdot p_\beta)^2} L_1(Q^2),\end{aligned}\quad (18)$$

for incoherent contribution, the "remaining" probability has to be considered for avoiding double counting, thus $L_1(Q^2)$ and $L_2(Q^2)$ take the following forms

$$L_1(Q^2) = L_2(Q^2) = 1 - G_E^2(Q^2). \quad (19)$$

For the inelastic reactions, the weighting factor is $P_\beta = 1 - G_E^2(Q^2)$. There are two types of photon contributions that should be considered: direct-photon contribution and resolved-photon contribution [9]. For the direct-photon process, the high-energy photon, emitted from the projectile interacts with the partons of target proton directly. For the resolved-photon process, the high-energy photon can fluctuate into a color singlet state with multiple $q\bar{q}$ pairs and gluons. Due to this fluctuation, the photon interacts with the partons in B like a hadron, and the subprocesses are almost the purely strong interaction processes. Together with the two different photon emissions mechanism mentioned earlier, we have four topologies: inelastic-coherent direct (inel-coh.dir.), inelastic-coherent resolved (inel-coh.res.), inelastic-incoherent direct (inel-incoh.dir.) and inelastic-incoherent resolved (inel-incoh.res.) processes. These abbreviations will appear in many places of remained content and we do not explain its meaning again. According to NRQCD factorization formalism, the cross section of J/ψ produced by inel-coh.dir. is

$$\begin{aligned}& \frac{d\sigma^{\text{inel-coh.dir.}}}{dQ^2}(p + p \rightarrow p + J/\psi + X) \\ &= \sum_b \int dy dx_b f_{b/p}(x_b, \mu^2) \sum_n \langle \mathcal{O}^{J/\psi}[n] \rangle \frac{d\sigma}{dydQ^2}(p + b \rightarrow p + c\bar{c}[n] + b),\end{aligned}\quad (20)$$

where $\langle \mathcal{O}^{J/\psi}[n] \rangle$ is the long-distance matrix elements of NRQCD. For inelastic reactions, $m_\beta = m_b = 0$, $x_b = p_b/p_B$ is the parton's momentum fraction, $f_{b/p}(x_b, \mu^2)$ is the parton distribution function of proton B. Based on Eq. (7), the cross section of subprocess $\alpha + b \rightarrow \alpha + c\bar{c}[n] + b$ should be rewritten as

$$\begin{aligned}
& \frac{d\sigma}{dydQ^2}(\alpha + b \rightarrow \alpha + c\bar{c}[n] + b) \\
&= \frac{e_\alpha^2 \alpha}{2\pi} \left[\frac{y\rho^{++}}{Q^2} \sigma_T(\gamma^* + b \rightarrow c\bar{c}[n] + b) + \frac{y\rho^{00}}{2Q^2} \sigma_L(\gamma^* + b \rightarrow c\bar{c}[n] + b) \right] P_\beta \\
& \quad \times f(s, p_{\text{CM}}, \hat{s}, \hat{p}_{\text{CM}}, m_\alpha, m_b) \\
&= dt \frac{e_\alpha^2 \alpha}{2\pi} F_b[n] \left[\frac{y\rho^{++}}{Q^2} T_b[n] - y\rho^{00} L_b[n] \right] P_\beta f(s, p_{\text{CM}}, \hat{s}, \hat{p}_{\text{CM}}, m_\alpha, m_b), \quad (21)
\end{aligned}$$

$F_b[n]$, $T_b[n]$ and $L_b[n]$ can be found in Refs. [29] and the proton tensor multiplied by Q^{-2} is

$$\begin{aligned}
\rho_{\text{inel-coh.}}^{++} &= H_2(Q^2) + \frac{1}{2} \left[\frac{(y-2)^2}{y^2} - \frac{4m_p^2}{Q^2} - 1 \right] H_1(Q^2), \\
\rho_{\text{inel-coh.}}^{00} &= -H_2(Q^2) + \frac{(y-2)^2}{y^2} H_1(Q^2). \quad (22)
\end{aligned}$$

In the same way, the cross section of J/ψ produced by inel-incoh.dir. reads

$$\begin{aligned}
& \frac{d\sigma^{\text{inel-incoh.dir}}}{dQ^2}(p + p \rightarrow X_A + J/\psi + X) \\
&= \sum_{a,b} \int dy dx_a dx_b f_{a/p}(x_a, \mu^2) f_{b/p}(x_b, \mu^2) \sum_n \langle \mathcal{O}^{J/\psi}[n] \rangle \\
& \quad \times \frac{d\sigma}{dydQ^2}(a + b \rightarrow a + c\bar{c}[n] + b), \quad (23)
\end{aligned}$$

the differential cross section $d\sigma/dy dQ^2(a + b \rightarrow a + c\bar{c}[n] + b)$ is the same as Eq. (21) but with $m_\alpha = 0$, the massless quark tensor multiplied by Q^{-2} is

$$\begin{aligned}
\rho_{\text{inel-incoh.}}^{++} &= [1 - G_E^2(Q^2)] \frac{1 + (1-y)^2}{y^2}, \\
\rho_{\text{inel-incoh.}}^{00} &= [1 - G_E^2(Q^2)] \frac{4(1-y)}{y^2}. \quad (24)
\end{aligned}$$

In the inelastic-coherent resolved process, the parton a' of hadron-like photon which emitted from proton A , interacts with the parton b of another incident proton B via the interactions of quark-antiquark annihilation, quark-gluon Compton scattering and gluon-gluon fusion. Therefore the cross section of J/ψ produced by inel-coh.res. has the form of

$$\begin{aligned}
& \frac{d\sigma^{\text{inel-coh.res.}}}{dQ^2}(p + p \rightarrow p + J/\psi + X) \\
&= \sum_b \sum_{a'} \int dy dx_b dz_{a'} d\hat{t} f_{b/p}(x_b, \mu^2) f_{a'/\gamma}(z_{a'}, \mu^2) \sum_n \langle \mathcal{O}^{J/\psi}[n] \rangle \\
&\times \frac{e_\alpha^2 \alpha y \rho_{\text{inel-coh.}}^{++}}{2\pi Q^2} \frac{d\sigma}{d\hat{t}}(a' + b \rightarrow c\bar{c}[n] + b), \tag{25}
\end{aligned}$$

where $z'_a = p_{a'}/q$ denotes the parton's momentum fraction of the resolved photon, $f_\gamma(z_{a'}, \mu^2)$ is the parton distribution function of the resolved photon [41], the complete list for the cross section of partonic processes $a' + b \rightarrow c\bar{c}[n] + b$ can be found in Refs. [42, 43]. The strong coupling constant is taken as the one-loop form [44]

$$\alpha_S = \frac{12\pi}{(33 - 2n_f) \ln(\mu^2/\Lambda^2)}, \tag{26}$$

with $n_f = 3$ and $\Lambda = 0.2$ GeV. In the inelastic-incoherent resolved process, the parton from hadron-like photon emitted by charged parton of incident proton can interact with the parton of target proton. The cross section of J/ψ produced by inel-incoh.res. has the form of

$$\begin{aligned}
& \frac{d\sigma^{\text{inel-incoh.res.}}}{dQ^2}(p + p \rightarrow X_A + J/\psi + X) \\
&= \sum_{a,b} \sum_{a'} \int dy dx_a dx_b dz_{a'} d\hat{t} f_{a/p}(x_a, \mu^2) f_{b/p}(x_b, \mu^2) f_{a'/\gamma}(z_{a'}, \mu^2) \sum_n \langle \mathcal{O}^{J/\psi}[n] \rangle \\
&\times e_a^2 \frac{\alpha y \rho_{\text{inel-incoh.}}^{++}}{2\pi Q^2} \frac{d\sigma}{d\hat{t}}(a' + b \rightarrow c\bar{c}[n] + b). \tag{27}
\end{aligned}$$

2.2. The p_T and z distributions of J/ψ production

It is straightforward to obtain the distributions of p_T and z by accordingly reordering and redefining the integration variables. For deriving the p_T distribution, the Mandelstam variables of partonic process $\gamma^* + \beta \rightarrow J/\psi + \beta$ should be written in the following forms

$$\begin{aligned}
\hat{s} &= 2 \cosh y_r m_T \sqrt{\cosh^2 y_r m_T^2 + m_\beta^2 - M_{J/\psi}^2} \\
&\quad + 2 \cosh^2 y_r m_T^2 + m_\beta^2 - M_{J/\psi}^2, \\
\hat{t} &= M_{J/\psi}^2 - Q^2 - 2m_T(E_q \cosh y_r - \hat{p}_{\text{CM}} \sinh y_r), \\
\hat{u} &= M_{J/\psi}^2 + m_\beta^2 - 2m_T(E_\beta \cosh y_r + \hat{p}_{\text{CM}} \sinh y_r),
\end{aligned} \tag{28}$$

where $y_r = (1/2) \ln(E + p_z)/(E - p_z)$ is the rapidity, $m_T = \sqrt{M_{J/\psi}^2 + p_T^2}$ is the J/ψ transverse mass, the expressions of E_q , E_β and \hat{p}_{CM} can be found in Appendix A. For elastic-coherent process, the variables y and \hat{t} should be transformed into the following form by using the Jacobian determinant

$$\begin{aligned}
d\hat{t}dy &= \mathcal{J}_{\text{el-coh.}} dy_r dp_T \\
&= \left| \frac{D(y, \hat{t})}{D(p_T, y_r)} \right| dy_r dp_T \\
&= \frac{2\hat{p}_{\text{CM}} \sqrt{\hat{s}} (\sqrt{\cosh^2 y_r m_T^2 + m_\beta^2 - M_{J/\psi}^2} + \cosh y_r m_T)}{(s_{\alpha\beta} - m_\alpha^2 - m_\beta^2) \sqrt{\cosh^2 y_r m_T^2 + m_\beta^2 - M_{J/\psi}^2}} dy_r dp_T,
\end{aligned} \tag{29}$$

the expressions of the Jacobian determinant for the rest processes are listed as follow

$$\begin{aligned}
\text{el - incoh. : } d\hat{t}dx_a &= \frac{\mathcal{J}_{\text{el-coh.}}}{y} dy_r dp_T, \\
\text{inel - coh.dir. : } d\hat{t}dx_b &= \frac{\mathcal{J}_{\text{el-coh.}}}{y} dy_r dp_T, \\
\text{inel - incoh.dir. : } d\hat{t}dx_b &= \frac{\mathcal{J}_{\text{el-coh.}}}{yx_a} dy_r dp_T, \\
\text{inel - coh.res. : } d\hat{t}dz_{a'} &= \frac{\mathcal{J}_{\text{el-coh.}}}{yx_b} dy_r dp_T, \\
\text{inel - incoh.res. : } d\hat{t}dz_{a'} &= \frac{\mathcal{J}_{\text{el-coh.}}}{yx_a x_b} dy_r dp_T,
\end{aligned} \tag{30}$$

For the z distribution, we can do the similar transformations, and the Mandelstam variables in Eq. (28) should be rewritten as: $\hat{s} = M_{J/\psi}^2/z + p_T^2/z(1-z)$, $\hat{t} = -(1-z)(\hat{s} + Q^2 - m_\beta^2)$ and $\hat{u} = M_{J/\psi}^2 + m_\beta^2 - z(\hat{s} + Q^2 - m_\beta^2)$.

2.3. The equivalent photon spectrum

The idea of EPA was first developed by Fermi [1], who replaced the electromagnetic fields from a fast-moving charged particle with an equivalent flux of photon. The number of photons with energy ω , $n(\omega)$, is given by the Fourier transform of the time-dependent electromagnetic field. Therefore, the electromagnetic interaction between the charged particle and the nucleus is reduced to the interaction between those photons and the nucleus. This idea has been extended to include the interaction of relativistic charged particles by Weizsäcker and Williams, and the method is often known as the Weizsäcker-Williams method [2]. An essential advantage of EPA consists in the fact that, when using it, it is sufficient to obtain the photo-absorption cross section on the mass shell only. Details of its off mass-shell behavior are not essential. Thus, the EPA approach, as a useful technique, has been widely applied to obtain various cross sections for charged particles production in relativistic heavy ion collisions [13].

Although tremendous successes have been achieved, the accuracy of EPA and its applicability range are often neglected, and a number of imprecise statements pertaining to the essence and the advantages of EPA were given [16, 20–25]. Some limitations of the kinematic variables are often used directly [17, 18, 29, 45–47], e.g., the choice of $Q_{\max}^2 \sim \hat{s}$ or ∞ is widely used instead of the significant dynamical cut off Λ_γ^2 which represents the precision of EPA [13]; $y_{\max} = 1$ is used in the calculations, actually it is far less than one in coherent or elastic processes; And the integration of some widely used spectra are performed over the entire kinematically allowed region, which leads to erroneous expressions. However, the exact treatment developed in the previous sections can reduce to the EPA when $Q^2 \rightarrow 0$. Detailed discussion on this issue can be also found in Ref. [13]. This provides us a powerful and overall approach for comparing our results with the EPA ones, to study the features of EPA in the entire kinematical ranges and give the appropriate kinematical relations.

Taking $Q^2 \rightarrow 0$, the transverse and longitudinal polarization tensors can

reduce to

$$\begin{aligned}\lim_{Q^2 \rightarrow 0} \varepsilon_L^{\mu\nu} &= -\frac{q^\mu q^\nu}{q^2}, \\ \lim_{Q^2 \rightarrow 0} \varepsilon_T^{\mu\nu} &= -g^{\mu\nu} + \frac{(q^\mu p_b^\nu + q^\nu p_b^\mu)}{q \cdot p_b}.\end{aligned}\quad (31)$$

Since $q^\mu T_{\mu\nu} = 0$, Eq. (7) becomes:

$$\begin{aligned}&\lim_{Q^2 \rightarrow 0} \frac{d\sigma}{dy dQ^2 d\hat{t}}(\alpha + \beta \rightarrow \alpha + J/\psi + \beta) \\ &= \left(e_\alpha^2 \frac{\alpha}{2\pi} \frac{y \rho^{++}}{Q^2} \right) \frac{d\sigma_T}{d\hat{t}}(\gamma^* + \beta \rightarrow J/\psi + \beta) \Big|_{Q^2=0} \\ &= \frac{df_\gamma(y)}{dQ^2} \frac{d\sigma_T}{d\hat{t}}(\gamma^* + \beta \rightarrow J/\psi + \beta) \Big|_{Q^2=0},\end{aligned}\quad (32)$$

where the general form of the equivalent photon flux function $f_\gamma(y)$ reads

$$\begin{aligned}f_\gamma(y) &= \int dQ^2 \frac{e_\alpha^2 \alpha}{2\pi} \frac{y \rho^{++}}{Q^2} \\ &= \frac{e_\alpha^2 \alpha}{2\pi} \int \frac{dQ^2}{Q^2} y \left[F_2(Q^2) + \left(\frac{2(1-y)}{y^2} - \frac{2m_\alpha^2}{Q^2} \right) F_1(Q^2) \right],\end{aligned}\quad (33)$$

we can see that the contribution of $d\sigma_L/d\hat{t}$ and the terms proportional to Q^2 are neglected in the limit $Q^2 \rightarrow 0$.

For the coherent case, there is a approximate analytic form which is developed by Drees and Zeppenfeld (DZ) [18], this photon flux of proton is widely used in the literatures [20–25]. By taking $Q_{\max}^2 \rightarrow \infty$, setting $F_1(Q^2) = F_2(Q^2) = G_E(Q^2)$ (which equals to neglect the contribution of magnetic form factor), and neglecting the m_α^2 term in Eq. (33), they obtained

$$f_\gamma^{\text{DZ}}(y) = \frac{\alpha}{2\pi} \frac{1 + (1-y)^2}{y} \left(\ln A - \frac{11}{6} + \frac{3}{A} - \frac{3}{2A^2} + \frac{1}{3A^2} \right), \quad (34)$$

where $A = (1 + 0.71 \text{ GeV}/Q_{\min}^2)$. For incoherent case, the complete form of photon flux can be derived from Eq. (33) by setting $F_1(Q^2) = F_2(Q^2) = 1 - G_E^2(Q^2)$ and $m_\alpha = 0$,

$$\begin{aligned}f_\gamma^{\text{incoh}}(y) &= \int dQ^2 \frac{\alpha}{2\pi} \frac{y \rho^{++}}{Q^2} \\ &= e_\alpha^2 \frac{\alpha}{2\pi} \frac{1 + (1-y)^2}{y} \int \frac{dQ^2}{Q^2} (1 - G_E^2(Q^2)).\end{aligned}\quad (35)$$

Actually, another approximate form of above equation is often used in the practical calculations [20–26], which neglects the second term of Eq. (35) and takes $Q_{\min}^2 = 1 \text{ GeV}^2$ and $Q_{\max}^2 = \hat{s}/4$

$$f_{\gamma}^{\text{incoh}}(y) = e_{\alpha}^2 \frac{\alpha}{2\pi} \frac{1 + (1 - y)^2}{y} \ln \frac{Q_{\max}^2}{Q_{\min}^2}. \quad (36)$$

3. Numerical results

In this section, we provide the numerical results for the J/ψ photoproductions in p-p UPCs at LHC energy. Several theoretical inputs and the kinematic conditions need to be provided. The mass of the proton and J/ψ are $m_p = 0.938 \text{ GeV}$, $m_{J/\psi} = 3.097 \text{ GeV}$ [49]. The long-distance matrix elements of NRQCD used in this paper can be found in Ref. [48], where

$$\begin{aligned} \langle \mathcal{O}^{J/\psi} [{}^3S_1^{(1)}] \rangle &= 1.2 \text{ GeV}^3, \\ \langle \mathcal{O}^{J/\psi} [{}^1S_0^{(8)}] \rangle &= 1.8 \times 10^{-2} \text{ GeV}^3, \\ \langle \mathcal{O}^{J/\psi} [{}^3S_1^{(8)}] \rangle &= 1.3 \times 10^{-3} \text{ GeV}^3, \end{aligned} \quad (37)$$

and the multiplicity relations

$$\begin{aligned} \langle \mathcal{O}^{J/\psi} [{}^3P_0^{(8)}] \rangle &= m_{\text{charm}}^2 \langle \mathcal{O}^{J/\psi} [{}^1S_0^{(8)}] \rangle, \\ \langle \mathcal{O}^{J/\psi} [{}^3P_J^{(8)}] \rangle &= (2J + 1) \langle \mathcal{O}^{J/\psi} [{}^3P_0^{(8)}] \rangle, \end{aligned} \quad (38)$$

are considered. We choose the MMHT2014 NNLO set for the parton distribution function of proton with $n_f = 3$ [50, 51]. The complete kinematical relations are given in Appendix A, one should note that the coherence condition [52] is considered for coherent reactions, which means that the wavelength of the photon is larger than the size of the nucleus, and the charged constituents inside the nucleus should act coherently. This condition limits Q^2 and y to very low value ($Q^2 \leq 1/R_A^2$, $R_A = A^{1/3}1.2 \text{ fm}$ is the size of the nucleus), $Q_{\max}^2 = 0.027 \text{ GeV}^2$ and $y_{\max} \sim 0.16$ for proton.

In Fig.2, the Q^2 distribution of J/ψ photoproduction in p-p UPCs is plotted. The curves of EPA and exact results share the same trend, and are consistent with each other in small Q^2 region, since EPA can be obtained from the exact treatment by setting $Q^2 \rightarrow 0$ and only considering the transverse

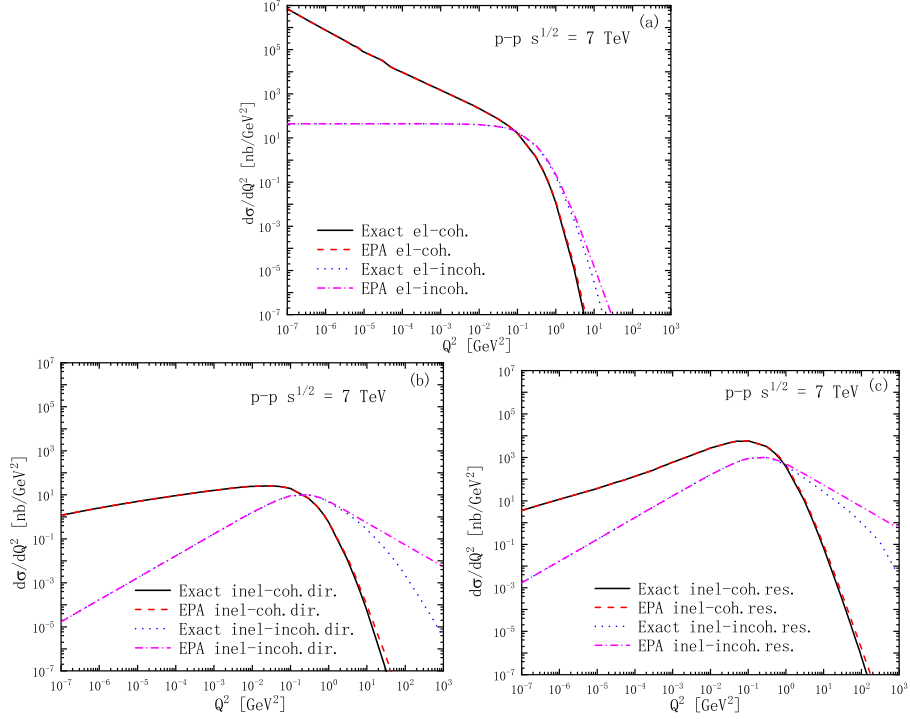


Figure 2: Comparisons of the exact results and the EPA ones for J/ψ photoproduction in p-p UPCs. (a): For elastic reactions, the solid (black) and dashed (red) lines represent the exact and EPA results of el-coh., respectively. The dotted (blue) and dashed-dotted (magenta) lines denote the exact and EPA results of el-incoh., respectively. (b): Same as (a) but for inelastic-direct processes. (c): Same as (a) but for inelastic-resolved processes.

photon contributions, this is one advantage of exact treatment. For the case of coherent photon emission processes, we can see that the contribution of el-coh. concentrates on the small Q^2 domain, and almost have no difference between exact result and the EPA one [Fig.2 (a)]. Inversely, the contribution of inel-coh. [Fig.2 (b),(c)] can be neglected in small Q^2 region compared to el-coh., and the difference between the exact result and the EPA one appears when $Q^2 > 1 \text{ GeV}^2$. For incoherent photon emission processes, its contributions are negligible by comparing with coherent ones in small Q^2 region and become larger when $Q^2 > 0.1 \text{ GeV}^2$, the difference between the exact results and the EPA ones are obvious, especially for inel-incoh. where the difference is prominent [Fig.2 (b),(c)]. Therefore, EPA is only applicable in the small Q^2 domain, this feature permits one to use it for coherent or elastic processes with proper choice of Q_{max}^2 , and reached the high precision. However, EPA is not a effective approximation for incoherent photon emission processes (especially for inel-incoh.), since its contribution dominate the large Q^2 region where the EPA errors are prominent.

Table 1: Total cross sections of the J/ψ photoproduction in the coherent channel.

	el-coh.			inel-coh.(dir.+res.)		
	σ [nb]	Δ^{a} [nb]	δ^{b} [%]	σ [nb]	Δ [nb]	δ [%]
Exact	13.3498	0.00	0.00	59.47	0.00	0.00
EPA CC ^c	13.3506	0.0008	0.00	59.49	0.02	0.00
EPA ($Q_{\text{max}}^2 \sim \hat{s}$)	19.2987	5.9489	44.56	92.20	32.73	55.03
EPA ($y_{\text{max}} = 1$)	22.3444	8.9946	67.38	106.83	47.37	79.64
EPA No WF	\	\	\	1152.6764	1093.20	1838.16

^a Absolute error with respect to the exact result: $\Delta = \sigma - \sigma_{\text{Exact}}$.

^b Relative error with respect to the exact result: $\delta = \Delta/\sigma_{\text{Exact}}$.

^c The EPA result with the coherence condition (CC).

To quantitatively estimate the EPA errors and discuss the influence from the different choice of kinematic limitations, we also calculate the total cross sections in Table 1 and 2. For coherent reactions in Table 1, we can see that the EPA results with coherence condition (CC) nicely agree with exact ones, since CC limits Q_{max}^2 and y_{max} to very low value which effectively cut the

Table 2: Total cross sections of the J/ψ photoproduction in the incoherent channel.

	el-incoh.			inel-incoh.(dir.+res.)		
	σ [nb]	Δ [nb]	δ [%]	σ [nb]	Δ [nb]	δ [%]
Exact	6.1573	0.00	0.00	422.75	0.00	0.00
EPA	6.3722	0.2149	3.49	1939.50	1516.75	358.78
EPA No WF	233.1243	226.9670	3686.14	9152.45	8729.70	2064.97
EPA ($Q_{\min}^2 \sim 1\text{GeV}^2$)	\	\	\	3941.85	3519.10	832.43

EPA errors. On the contrary, the usual choice of $Q_{\max}^2 \sim \hat{s}$ and $y_{\max} = 1$ in most literatures bring the large errors. For incoherent reactions in Table 2, the EPA error is not obvious in el-incoh., since the elastic interactions dominate the very small Q^2 region which effectively suppresses the EPA errors. Unlikely el-incoh., the EPA error of inel-incoh. are prominent, which verifies again that the essence of incoherent photon emission processes is in contradiction with the feature of EPA. Besides, we can see that the coherent and incoherent reactions are the main channel of elastic and inelastic interactions, respectively. It should be emphasized that, if the Martin-Ryskin method is not considered, the contribution of incoherent and inelastic reactions will always much larger than coherent and elastic reactions in the whole Q^2 region. This unphysical result is caused by the double counting, and is most serious in inel-incoh.. Comparing with Martin-Ryskin method which avoid this unphysical large value naturally, the results obtained by using the artificial cutoff $Q_{\min}^2 = 1$ GeV, which is widely applied in the literatures [20–26], still have large errors ($\delta \sim 832\%$).

In Fig.3, the z distribution of J/ψ photoproduction in p-p UPCs is plotted. The EPA results nicely agree with exact ones in coherent reactions in the whole z regions. But in the incoherent reactions, the difference between the exact results and EPA ones are significant, about an order of magnitude. For elastic interactions [Fig.3(a)], the curves is negligible in the most regions of z and become important when $z > 0.9$, especially near $z = 1$, the curves show a pronounced peak. For the case of inelastic interactions [Fig.3(b),(c)], the contributions are important in the most of z regions. The curves of

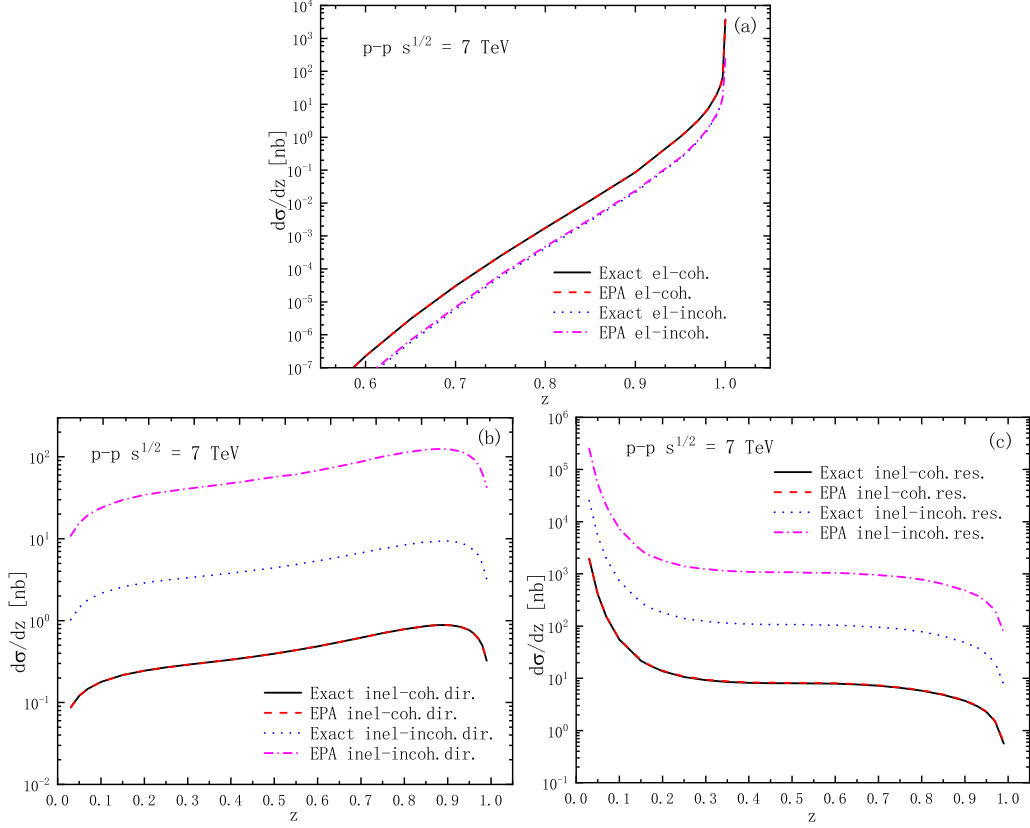


Figure 3: The z distribution of J/ψ photoproduction in p-p UPCs. (a): The elastic reactions. (b): The inelastic-direct processes, the solid (black), dashed (red) and dotted (blue) lines represent the inel-coh.dir. results of exact treatment, EPA and EPA without WF factors, respectively; those for inel-incoh.dir. are depicted by the same type lines but are bolded and with different colors. (c): Same as (b) but for inelastic-resolved processes.

inelastic-direct processes is comparable with elastic reactions near $z = 0.9$, but rapidly decreased near $z = 1$. These features are in agreement with the traditional perspective that $z = 0.9$ is the boundary to distinguish the elastic and inelastic reactions. Finally, for the case of inelastic-resolved processes, its contribution dominate the region $z < 0.2$.

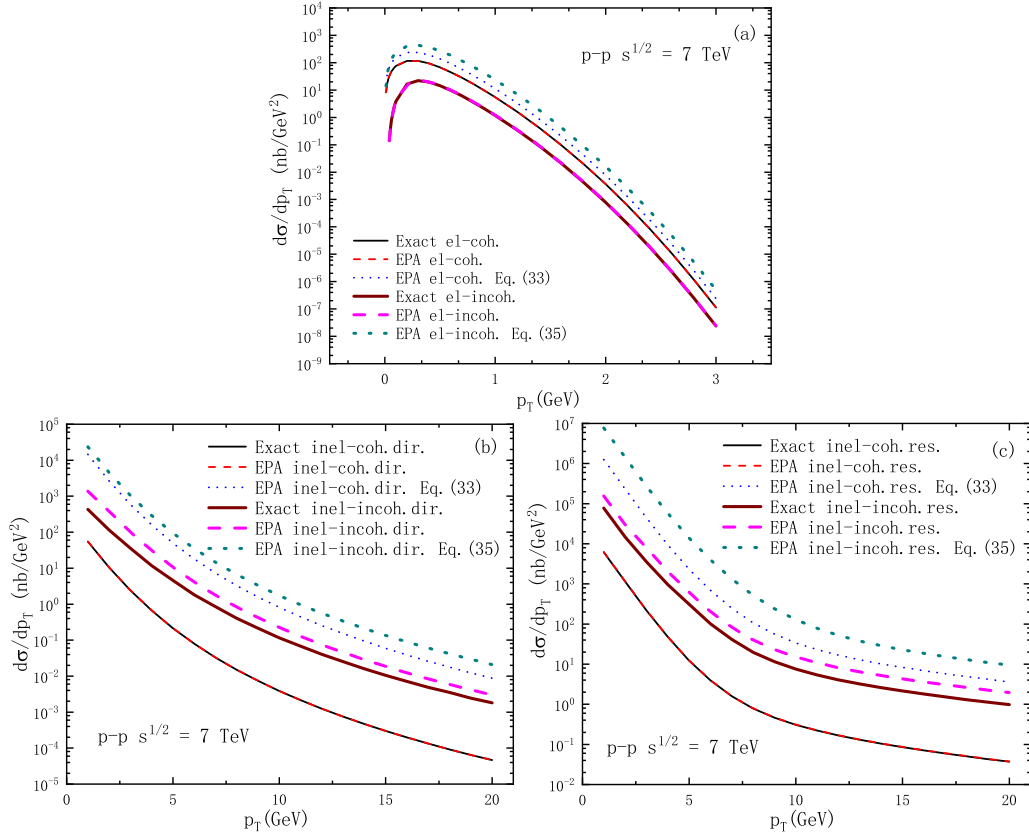


Figure 4: The p_T distribution of J/ψ photoproduction in p-p UPCs. (a): The elastic reactions, the solid (black), dashed (red) and dotted (blue) lines represent the el-coh. results of exact treatment, EPA and EPA with Eq. (33), respectively; those for el-incoh. are depicted by the same type lines but are bolded and with different colors. (b): Same as (a) but for inelastic-direct processes. (c): Same as (a) but for inelastic-resolved processes.

In Fig.4, the p_T distribution of J/ψ photoproduction in p-p UPCs is plotted, the equivalent photon fluxes Eqs.(34) and (36) are discussed. For the case of coherent reactions, the exact results nicely agree with the EPA ones in the whole p_T region, since the coherence condition is adopted in

the calculations. However, the results based on the equivalent photon flux function Eq.(34) are much larger than the results of exact treatment, since $Q_{\max}^2 = \infty$ is adopted in Eq.(34), which causes the large EPA errors. For the case of incoherent reactions, the EPA results are greater than the exact one in the whole p_T region, but the difference between the EPA result Eq. (36) and the exact one is much more evident (especially for the inel-incoh.res. in Fig.4 (c)), since $Q_{\max}^2 = \hat{s}/4$ is employed in Eq.(36), which include the large fictitious contribution from the large Q^2 domain. Otherwise, the option $y_{\max} = 1$ is used directly in these two fluxes, which is another important sources of errors. Therefore, the choice of Q_{\max}^2 and y_{\max} are crucial to the accuracy of EPA, and the results based on Eq.(34) and (36) are not accurate enough. For dealing with the incoherent processes, the exact treatment has to be considered.

4. Summary and conclusions

In this paper, we calculate the J/ψ photoproduction in p-p Ultra-peripheral collisions at LHC energy. The elastic and inelastic interactions, and coherent and incoherent photon emission processes are considered simultaneously. The exact treatment, which can reduce to EPA in the limit $Q^2 \rightarrow 0$, is developed, where the proton or quark tensor is expanded by using the transverse and longitudinal polarization operators, and the square of electric form factor $G_E^2(Q^2)$ is used as weighting factor for avoiding double counting. Otherwise, the full kinematical relations are also achieved. In order to study the feature of EPA in the entire kinematical ranges, the comparisons between the exact results and the EPA ones are expressed as the Q^2 , z and p_T distributions, and total cross sections are also estimated.

The numerical results indicate that the EPA is only applicable in a very restricted domain (small y and Q^2 domain), and is very sensitive to the value of y_{\max} and Q_{\max}^2 , this feature permits one to use it for coherent or elastic processes with appropriate choice of Q_{\max}^2 and y_{\max} , and reached the high precision. Coherence condition is a good choice which effectively cut the errors from large y and Q^2 domain. The common options $Q_{\max}^2 \sim \hat{s}$ or ∞ , and $y_{\max} = 1$ will cause the large errors. Besides, the validity condition of EPA is in contradiction with the essence of incoherent photon emission processes (especially for inel-incoh.), where the serious double counting problem also exist. Therefore, EPA can not provide accurate enough results for J/ψ photoproduction in p-p Ultra-peripheral collisions, and the exact treatment needs

to be adopted which has the widely applicability range and can naturally avoid double counting.

Acknowledgements

This work is supported in part by National Key R & D Program of China under grant No. 2018YFA0404204, the National Natural Science Foundation of China (Grant Nos. 11747086 and 11575043), and by the Young Backbone Teacher Training Program of Yunnan University. Z. M. is supported by Yunnan Provincial New Academic Researcher Award for Doctoral Candidates.

Appendix A. Full kinematical relations

For the Q^2 distribution, the bounds of integration variables for elastic-coherent process are given by

$$\begin{aligned}
\hat{t}_{\min} &= M_{J/\psi}^2 - Q^2 - 2(E_q E_{J/\psi} + p_{\text{CM}} p'_{\text{CM}}), \\
\hat{t}_{\max} &= M_{J/\psi}^2 - Q^2 - 2(E_q E_{J/\psi} - p_{\text{CM}} p'_{\text{CM}}), \\
y_{\min} &= \frac{\hat{s}_{\min} + Q^2 - m_\beta^2}{s - m_\alpha^2 - m_\beta^2}, \\
y_{\max} &= \frac{1}{2m_\alpha^2} \left(\frac{\sqrt{Q^2(4m_\alpha^2 + Q^2)[(s - m_\alpha^2 - m_\beta^2)^2 - 4m_\alpha^2 m_\beta^2]}}{s - m_\alpha^2 - m_\beta^2} - Q^2 \right),
\end{aligned} \tag{A.1}$$

where $s_{\min} = (M_{T\min} + p_{T\min})^2$, s is the energy square of p-p CM frame, $y_{\max(\min)}$ is same for all kinds of reactions and not list in the following again, the energy and momentum in $\gamma^*\beta$ CM frame are

$$\begin{aligned}
E_q &= \frac{1}{2\sqrt{\hat{s}}}(\hat{s} - Q^2 - m_\beta^2), \\
E_{J/\psi} &= \frac{1}{2\sqrt{\hat{s}}}(\hat{s} + M_{J/\psi}^2 - m_\beta^2), \\
\hat{p}_{\text{CM}} &= \frac{1}{2\sqrt{\hat{s}}}\sqrt{(\hat{s} + Q^2 - m_\beta^2)^2 + 4Q^2 m_\beta^2},
\end{aligned}$$

$$\hat{p}'_{\text{CM}} = \frac{1}{2\sqrt{\hat{s}}} \sqrt{(\hat{s} - M_{J/\psi}^2 - m_\beta^2)^2 - 4M_{J/\psi}^2 m_\beta^2}, \quad (\text{A.2})$$

For the elastic-incoherent case, the bounds of variables are the same as Eq. (A.1), but for $x_{\text{amin}} = (\hat{s}_{\text{min}} + Q^2 - m_\beta^2)/y(s_{\alpha\beta} - m_\alpha^2 - m_\beta^2)$, $x_{\text{amax}} = 1$. The bounds of variables for inelastic interactions are given in Table A.3.

Table A.3: The bounds of variables for inelastic interactions. $\hat{s}_{\text{min}} = \hat{s}_{\gamma\text{min}}$, $p_T^2 = \hat{t}(\hat{s}\hat{u} + Q^2 M^2)/(\hat{s} + Q^2)^2$ and $\hat{t}_\gamma \hat{u}_\gamma / \hat{s}_\gamma$ for inelastic-direct and -resolved process, respectively.

variables	coh.dir	incoh.dir	coh.res	incoh.res
$z_{q\text{min}}$		$\frac{M_{J/\psi}^2 + \hat{s}}{2\hat{s}} - \frac{\sqrt{(\hat{s} - M_{J/\psi}^2)^2 - 4p_{T\text{min}}^2 \hat{s}}}{2\hat{s}}$		
$z_{q\text{max}}$		$\frac{M_{J/\psi}^2 + \hat{s}}{2\hat{s}} + \frac{\sqrt{(\hat{s} - M_{J/\psi}^2)^2 - 4p_{T\text{min}}^2 \hat{s}}}{2\hat{s}}$		
\hat{t}_{min}		$(z_{q\text{min}} - 1)(\hat{s} + Q^2)$		$(z'_{q\text{min}} - 1)\hat{s}_\gamma$
\hat{t}_{max}		$(z_{q\text{max}} - 1)(\hat{s} + Q^2)$		$(z'_{q\text{max}} - 1)\hat{s}_\gamma$
$z_{a'\text{min}}$	\	\	$\frac{\hat{s}_{\gamma\text{min}}}{yx_b(s-2m_p^2)}$	$\frac{\hat{s}_{\gamma\text{min}}}{yx_a x_b(s-2m_p^2)}$
$z_{a'\text{max}}$	\	\	1	1
$x_{b\text{min}}$	$\frac{\hat{s}_{\text{min}} + Q^2}{y(s-2m_p^2)}$	$\frac{\hat{s}_{\text{min}} + Q^2}{yx_a(s-2m_p^2)}$	$\frac{\hat{s}_{\gamma\text{min}}}{z_{a\text{max}}y(s-2m_p^2)}$	$\frac{\hat{s}_{\gamma\text{min}}}{z_{a\text{max}}yx_a(s-2m_p^2)}$
$x_{b\text{max}}$			1	
$x_{a\text{min}}$	\	$\frac{\hat{s}_{\text{min}} + Q^2}{y(s-2m_p^2)}$	\	$\frac{\hat{s}_{\gamma\text{min}}}{z_{a\text{max}}y(s-2m_p^2)}$
$x_{a\text{max}}$	\	1	\	1

For the p_T distribution, the bounds of y , x_a and x_b are the same as Q^2 distribution, but for $z_{a'\text{max}} = 1/(1 + Q^2/4p_T^2)$ [53, 54]. And instead of \hat{t} , Q^2 and y_r should be integrated out

$$Q^2_{\text{min}}| = \frac{x_1^2}{1 - x_1} m_\alpha^2,$$

$$\begin{aligned}
Q_{\max}^2|_{\text{coh}} &= 0.027 \text{ GeV}^2, \quad Q_{\max}^2|_{\text{incoh}} = (1 - x_1)s, \\
|y_{r\max}| &= \\
\frac{1}{2} \ln &\frac{\hat{s}_{\max} + M_{J/\psi}^2 - m_\beta^2 + \sqrt{(\hat{s}_{\max} - M_{J/\psi}^2 - m_\beta^2)^2 - 4(M_{J/\psi}^2 m_\beta^2 + p_T^2 \hat{s}_{\max})}}{\hat{s}_{\max} + M_{J/\psi}^2 - m_\beta^2 - \sqrt{(\hat{s}_{\max} - M_{J/\psi}^2 - m_\beta^2)^2 - 4(M_{J/\psi}^2 m_\beta^2 + p_T^2 \hat{s}_{\max})}},
\end{aligned} \tag{A.3}$$

where $x_1 = \hat{s}/s$.

For the z distribution, the bounds of variables are the same as Q^2 distribution, but instead of \hat{t} , Q^2 should be integrated out and its bounds are the same as Eq. (A.3).

References

- [1] E. Fermi, Z. Phys. **29**, 315-327 (1924).
- [2] C. F. von Weizsacker, Z. Phys. **88**, 612-625 (1934).
- [3] E. J. Williams, Phys. Rev. **45**, 729 (1934).
- [4] L.D. Landau and E.M. Lifshitz, Sov. Phys. **6**, 244 (1934).
- [5] G. Nordheim et al., Phys. Rev. **51**, 1037 (1937).
- [6] R. H. Dalitz and D. R. Yennie, Phys. Rev. **105**, 1598 (1957).
- [7] I. Ya. Pomeranchuk and I. M. Shmushkevich, Nucl. Phys. **23**, 1295 (1961).
- [8] R. B. Curtis, Phys. Rev. **104**, 211 (1956).
- [9] Z. L. Ma and J. Q. Zhu, Phys. Rev. D **97**, no.5, 054030 (2018).
- [10] Z. L. Ma, Z. Lu, J. Q. Zhu and L. Zhang, [arXiv:1910.04509 [hep-ph]].
- [11] J. Nystrand, Nucl. Phys. A **752**, 470-479 (2005).
- [12] J. Nystrand, Nucl. Phys. A **787**, 29-36 (2007).
- [13] V. M. Budnev, I. F. Ginzburg, G. V. Meledin and V. G. Serbo, Phys. Rept. **15**, 181-281 (1975).

- [14] S. J. Brodsky, T. Kinoshita and H. Terazawa, Phys. Rev. D **4**, 1532-1557 (1971).
- [15] H. Terazawa, Rev. Mod. Phys. **45**, 615-662 (1973).
- [16] J. Q. Zhu, Z. L. Ma, C. Y. Shi and Y. D. Li, Nucl. Phys. B **900**, 431-445 (2015).
- [17] M. Drees, J. R. Ellis and D. Zeppenfeld, Phys. Lett. B **223**, 454-460 (1989).
- [18] M. Drees and D. Zeppenfeld, Phys. Rev. D **39**, 2536 (1989).
- [19] S. Frixione, M. L. Mangano, P. Nason and G. Ridolfi, Phys. Lett. B **319**, 339-345 (1993).
- [20] J. Q. Zhu, Z. L. Ma, C. Y. Shi and Y. D. Li, Phys. Rev. C **92**, no.5, 054907 (2015).
- [21] G. M. Yu and Y. D. Li, Phys. Rev. C **91**, no.4, 044908 (2015).
- [22] G. M. Yu, Y. C. Yu, Y. D. Li and J. S. Wang, Nucl. Phys. B **917**, 234-240 (2017).
- [23] G. M. Yu, Y. B. Cai, Y. D. Li and J. S. Wang, Phys. Rev. C **95**, no.1, 014905 (2017).
- [24] Y. P. Fu and Y. D. Li, Nucl. Phys. A **865**, 76-82 (2011).
- [25] Y. P. Fu and Y. D. Li, Chin. Phys. C **36**, 721-726 (2012).
- [26] Y. P. Fu and Y. D. Li, Phys. Rev. C **84**, 044906 (2011).
- [27] D. Graudenz, Phys. Rev. D **49**, 3291-3319 (1994).
- [28] S. Fleming and T. Mehen, Phys. Rev. D **57**, 1846-1857 (1998).
- [29] B. A. Kniehl and L. Zwirner, Nucl. Phys. B **621**, 337-358 (2002).
- [30] A. D. Martin and M. G. Ryskin, Eur. Phys. J. C **74**, 3040 (2014).
- [31] G. Baur, K. Hencken and D. Trautmann, J. Phys. G **24**, 1657-1692 (1998).

- [32] G. T. Bodwin, E. Braaten and G. P. Lepage, Phys. Rev. D **51**, 1125-1171 (1995) [erratum: Phys. Rev. D **55**, 5853 (1997)].
- [33] H. G. Dosch and E. Ferreira, Phys. Lett. B **576**, 83-89 (2003).
- [34] A. Di Giacomo, H. G. Dosch, V. I. Shevchenko and Y. A. Simonov, Phys. Rept. **372**, 319-368 (2002).
- [35] H. G. Dosch, E. Ferreira and A. Kramer, Phys. Rev. D **50**, 1992-2015 (1994).
- [36] H. G. Dosch, T. Gousset, G. Kulzinger and H. J. Pirner, Phys. Rev. D **55**, 2602-2615 (1997).
- [37] C. Ewerz and O. Nachtmann, Annals Phys. **322**, 1635-1669 (2007).
- [38] O. Nachtmann, Annals Phys. **209**, 436-478 (1991).
- [39] H. G. Dosch, Phys. Lett. B **190**, 177-181 (1987).
- [40] H. G. Dosch and Y. A. Simonov, Phys. Lett. B **205**, 339-344 (1988).
- [41] M. Gluck, E. Reya and I. Schienbein, Phys. Rev. D **60**, 054019 (1999) [erratum: Phys. Rev. D **62**, 019902 (2000)].
- [42] M. Klasen, B. A. Kniehl, L. N. Mihaila and M. Steinhauser, Phys. Rev. D **68**, 034017 (2003).
- [43] M. Klasen, B. A. Kniehl, L. N. Mihaila and M. Steinhauser, Phys. Rev. D **77**, 117501 (2008)..
- [44] Z. L. Ma, J. Q. Zhu, C. Y. Shi and Y. D. Li, Chin. Phys. Lett. **32**, no.12, 121202 (2015).
- [45] M. Drees, R. M. Godbole, M. Nowakowski and S. D. Rindani, Phys. Rev. D **50**, 2335-2338 (1994).
- [46] B. A. Kniehl, Phys. Lett. B **254**, 267-273 (1991) doi:10.1016/0370-2693(91)90432-P
- [47] A. Winther, K. Alder, Nucl. Phys. A **319**, 518 (1979); C. A. Bertulani, G. Baur, Nucl. Phys. A **442**, 739 (1985); C. A. Bertulani, G. Baur, Nucl. Phys. A **458**, 725 (1986); E. Papageorgiu, Phys. Lett. B **250**, 155 (1990).

- [48] R. Sharma and I. Vitev, Phys. Rev. C **87**, no.4, 044905 (2013).
- [49] K. A. Olive *et al.* [Particle Data Group], Chin. Phys. C **38**, 090001 (2014)
- [50] L. A. Harland-Lang, A. D. Martin, P. Motylinski and R. S. Thorne, Eur. Phys. J. C **75**, no.5, 204 (2015).
- [51] L. A. Harland-Lang, A. D. Martin, P. Motylinski and R. S. Thorne, Eur. Phys. J. C **75**, no.9, 435 (2015).
- [52] G. Baur, K. Hencken, D. Trautmann, S. Sadovsky and Y. Kharlov, Phys. Rept. **364**, 359-450 (2002).
- [53] G. Rossi, Phys. Rev. D **29**, 852 (1984).
- [54] M. Gluck, E. Reya and M. Stratmann, Phys. Rev. D **51**, 3220-3229 (1995).